JOURNAL OF MATERIALS SCIENCE 40 (2005) 5381–5386

Interfacial micromechanics of technora fibre/epoxy composites

WARAWAN PRASITHPHOL, ROBERT J. YOUNG
Materials Science Centre, School of Materials, University of Manchester, Grosvenor Street, Manchester M1 7HS, UK

The application of Raman spectroscopy using a near-infrared laser (IR) for the study of the deformation micromechanics of Technora fibres and single Technoras fibre embedded in epoxy composites is reported. The shift with strain of the Raman band approximately at 1613 cm^{-1} corresponding to *p*-phenylene ring deformation is studied. It is shown that the shift of the Raman band can be used to monitor the deformation micromechanics of the Technora/epoxy composites allowing the interfacial shear stress (ISS) to be determined. It was found that the maximum ISS was close to the shear yield stress of the resin indicating that there is good adhesion between the Technora fibres and the epoxy resin matrix.

1. Introduction

Technora fibres are high performance fibres having the chemical structure shown in Fig. 1. The fibres have high strength and high modulus, and also good chemical and impact resistance [1] which makes them suitable for composite reinforcements.

Raman spectroscopy has been used for the study of the deformation micromechanics of polymeric fibres and their composites [2–7]. The technique involves with the observation that the Raman bands corresponding to the vibrational modes of bonds in the fibre shift towards lower wavenumber with tension, thought to be due to direct molecular deformation [8]. This has been used to map strains along aramid fibres embedded in matrix resins to determine interfacial shear stress of the composites [2, 4, 5]. Interfacial adhesion between the fibres and matrices in the composites can be determined using Raman spectroscopy with a variety of specimen geometries such as the pull-out test, push-in test, microbond test and fragmentation geometry.

The aim of this paper is to illustrate that a well-defined Raman spectrum of a Technora fibre can be obtained using a near-IR laser and further to investigate the strength of interfacial adhesion in Technora fibre/epoxy resin composite system using Raman spectroscopy.

2. Experimental details

2.1. Materials

The Technora fibres, which have a yellow-gold colour, were supplied by Teijin-Twaron Ltd., Japan. A cold-curing epoxy resin system (LY5052/HY5052 in a ratio of 100/38 parts by weight), supplied by Ciba Geigy, UK, was used as the composite matrix.

2.2. Single fibre deformation

The single fibres were prepared for deformation by fixing on a window card using cyanoacrylate adhesive. After that, the specimens were conditioned in a temperature-controlled room at 50 ± 5% humidity and 23 ± 2°C for 7 days for the adhesive to be completely cured prior to testing.

The mechanical properties of all specimens were then determined for different gauge lengths in the temperature-controlled room using an Instron 1121 universal testing machine following ASTM D3379-75 with a cross-head speed of 1 mm/min. The Instron machine was calibrated using a standard weight of 1 N before testing. At least ten samples were tested, and average values and standard deviation of mechanical properties were calculated. The stress on the fibres was determined from the load using the fibre diameter obtained from the measurement using scanning electron microscopy (SEM) with gold-coated fibres using an excitation voltage of 2 keV.

2.3. Raman spectroscopy

Single fibres were also deformed using a stressing rig placed under the microscope of the Renishaw 1000 Raman spectrometer. The specimen was placed on the sample stage and illuminated by the ×50 objective lens. It was then irradiated by the laser beam and the ×50 objective lens used again to collect the scattered beam. A light-sensitive charge-coupled device, CCD, was used to collect the Raman spectra. The experimental results were analysed using a computer connected to the Raman spectrometer with the GRAMS-32™ software package. Raman spectra were obtained using an exposure time of 3 s at each strain level until the fibre failed and at least 3 samples were tested. Finally, the

0022-2461
DOI: 10.1007/s10853-005-4335-z

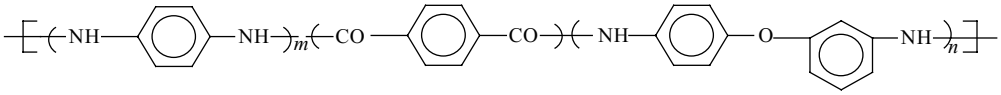

Figure 1 Chemical structure of the Technora molecule, the copolyamide of terephthaloyl chloride, p-phenylenediamine and 3,4′-diaminodiphenyl-ether (Technora fibre) where m and n are mol percents and $m + n = 100$ %. The mole fraction of 3,4′-diaminodiphenyl ether, n, is at least 30% and probably 50%.

shift of the Raman band with strain was then obtained and used as a strain calibration for composite testing. For the majority of the measurements a near-infrared (IR) laser with the wavelength of 785 nm, an exposure time 3 s and a single accumulation time were employed. The band intensity and band position were analysed by fitting to a Lorentzian function. An attempt was also made to obtain a Raman spectrum from the Technora fibres using a HeNe laser of wavelength 632 nm.

2.4. X-ray photoelectron spectroscopy (XPS)

The XPS measurements were carried out at the Corrosion and Protection Centre, School of Materials, University of Manchester. A bundle of Technora fibres for XPS analysis was clamped on to a rectangular sample holder. The XPS instrument used was an AXIS ULTRA from Kratos Analytical Ltd., operated at 150 W. The samples exposed to AlK_α X-rays to obtain the spectra. The machine was set to scan across a 20 eV range with a step size of 0.05 eV and a pass energy of 40 eV. Casa XPS software was used to determine the atomic percentage of the elements in the surface of the fibres.

2.5. Composite micromechanics

Single fibre model composites were prepared using 100 parts by weight of LY 5052, Araldite resin and 38 parts by weight of HY 5052, hardener. A mixture of resin/hardener was well mixed and degassed in a vacuum oven before being poured into the mould. After that the mixture was poured onto a 22 × 22 cm metal mould covered by translucent Mylar™ sheet to facilitate release of the composite sheets from the mould. The mixture was left for 1 h to cure partially. The fibres were cut to a length of 2–3 mm by ceramic scissors and placed onto the surface of the resin. Another batch of the resin mixture was prepared and poured onto the mould to sandwich the previously-prepared mixture and then left to cure for 7 days at room temperature. Having been removed from the mould, the composite sheet was cut by a band saw into strips with the fibre in the middle, which were then cut into dumbbell specimens. The surfaces of the specimen were polished to 3 mm thickness by the grinding machine. The edges were smoothed using fine sand paper. A resistance strain gauge with a gauge factor of 2.065 was mounted on the specimen using cyanoacrylate adhesive and left to cure for 2 h. After that, two wires were fixed onto the strain gauge using solder.

The model composites were deformed using a Minimat straining rig. The strains on the composites were monitored using the strain gauges. The matrix strain was calculated from the strain gauges using a digital multimeter. The Minimat, with a specimen mounted, was attached to the stage of the microscope so that the fragmentation could be observed simultaneously as the load was increased. The laser beam was focused to the fibre inside the resin matrix using a ×50 objective lens and the near-IR laser operated with an exposure time of 3 s and five accumulations was used. The shift of 1613 cm^{-1} Raman band along the length of the fibre at each level of matrix strain applied was examined. The matrix strain was increased in increments from 0 to 0.5, 1.0 and 1.5%. The measurements were taken at every 10 μm at both ends of the fibre and every 40 μm along the middle of the fibres. At least 3 samples were tested to obtain the average values of interfacial shear stress and standard deviations.

3. Results and discussion

3.1. Diameter measurements

The fibres were found to have approximately circular cross-sections and the average diameters of the fibres are illustrated in Table I. The standard deviation may be a result of the production of the fibres or the coating processes, but also may be from the errors in the SEM measurements and the assumption of a circular diameter.

3.2. Mechanical properties of Technora fibres

The mechanical properties of reinforcing fibres have a great influence on composite properties for load carrying applications. A typical stress/strain curve of a Technora fibre is illustrated in Fig. 2. The fibre Young's modulus, E_f, is found to depend on degree of polymer chain orientation [9] and the increase of the slope at higher strains is due to the improvement in orientation with increasing strain [9]. Summaries of mechanical properties (E_f, tensile strength, σ_f^*, and failure stain, e_f^*) of the Technora fibres are given in Table I.

3.3. Raman spectroscopy and single fibre deformation

The Raman spectra of the Technora fibres obtained using the He/Ne and near-IR lasers are shown in Fig. 3. It

TABLE I Diameters and mechanical properties of Technora fibres

Fibre	Diameter (μm)	Extrapolated[a] value of E_f (GPa)	Extrapolated[b] value of σ_f^* (GPa)	Extrapolated[a] value of e_f^* (%)
Technora	12.6 ± 0.5	96.4 ± 6.5	3.6 ± 0.3	4.1 ± 0.2

[a]Extrapolated to infinite gauge length.
[b]Extrapolated to zero gauge length.

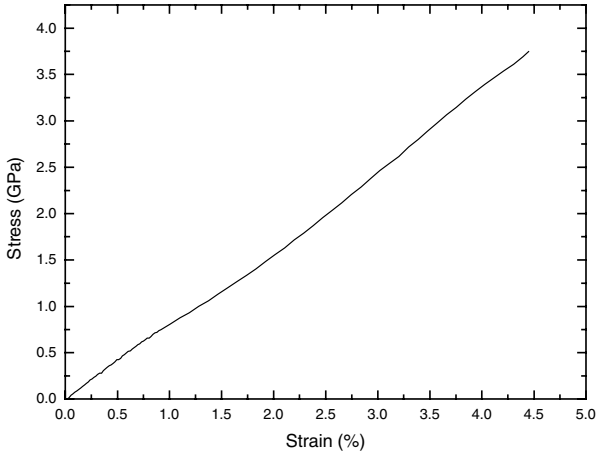

Figure 2 Stress/strain curve of a Technora fibre.

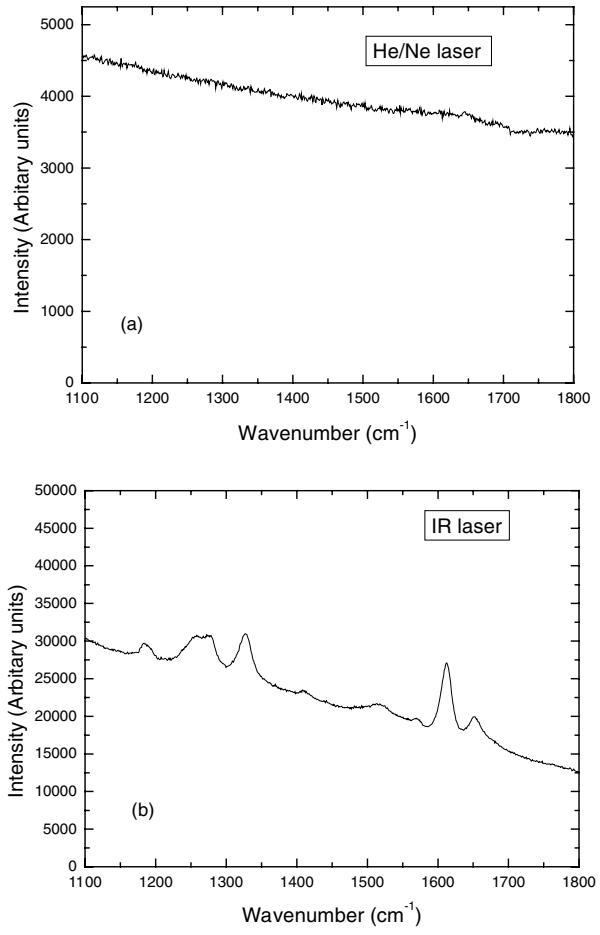

Figure 3 Raman spectrum of single Technora fibres obtained using the (a) He/Ne and (b) the IR lasers.

can be seen that no well-defined peaks are found for the HeNe laser but that a well-defined Raman spectrum of Technora fibre can be obtained using the near-IR laser. It appears that the use of the near-IR laser overcomes fluorescence problems encountered for this fibre with visible lasers and the band assignments are given in Table II. The shift with Technora fibre strain for the Raman band at approximately 1613 cm^{-1}, which is assigned to benzene ring deformation [12], is shown in Fig. 4. It can be seen that the peak shifts to lower wavenumber with tensile strain. This is because of the

TABLE II Raman band assignments for the Technora fibre [11]

Peak	Peak assignments
1653	C=O stretching, C–N stretching
1613	C–C ring stretching
1518	Ring C–H in plane bending, C=O stretching
1328	Ring C–H in plane bending
1274	N–H in-plane bending
1260	C–O stretching, N–H stretching
1183	Ring C–H in plane bending

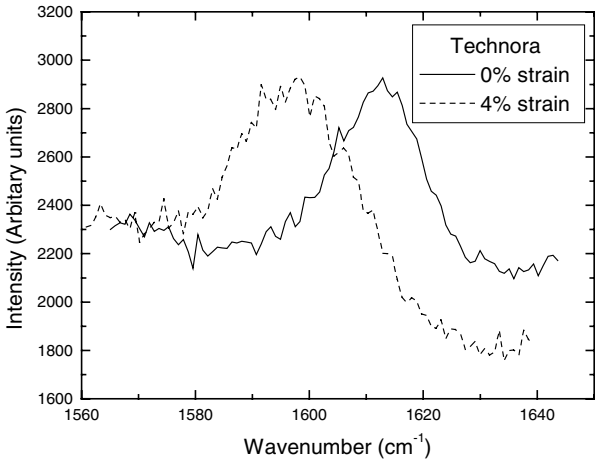

Figure 4 The shift of the 1613 cm^{-1} Raman band of a free-standing single Technora fibre at different strain levels.

asymmetry of the interatomic potential function leads to a change in the force constant with strain [10].

It was found that this Raman band shifts approximately linearly with strain to lower wavenumber (Fig. 5a); the average slope value obtained between 0 and 3% strain was determined to be -3.6 ± 0.1 cm^{-1}/%. Fig. 5b shows that the rate of shift of the Raman band with stress is -4.0 ± 0.1 cm^{-1}/GPa which is typical of other high-modulus fibres with *p*-substitute benzene rings in the main chain [12]. Due to its highest intensity, large stress-induced shift, and the lack of any significant fluorescence or significant Raman scattering from the epoxy resin, the 1613 cm^{-1} band was used to follow the deformation of the Technora fibre embedded in the composite.

3.4. X-Ray photoelectron spectroscopy (XPS) of Technora fibres

XPS has been used in this research to determine the elemental compositions of any finishing agents present on the surface of the fibres. In XPS, the samples are irradiated by soft X-rays causing electrons to be ejected. The binding energy, which may be regarded as the energy difference between the initial and final states after the photoelectron has left the atom, is a characteristic of the atom from which the electron was emitted thus each element has a unique spectrum [13].

The atomic percentage of element son the surface of the Technora fibres is illustrated in Table III. The atomic percentage of Technora fibres differs from the theoretical values indicating that the fibres had been treated with finishing agents.

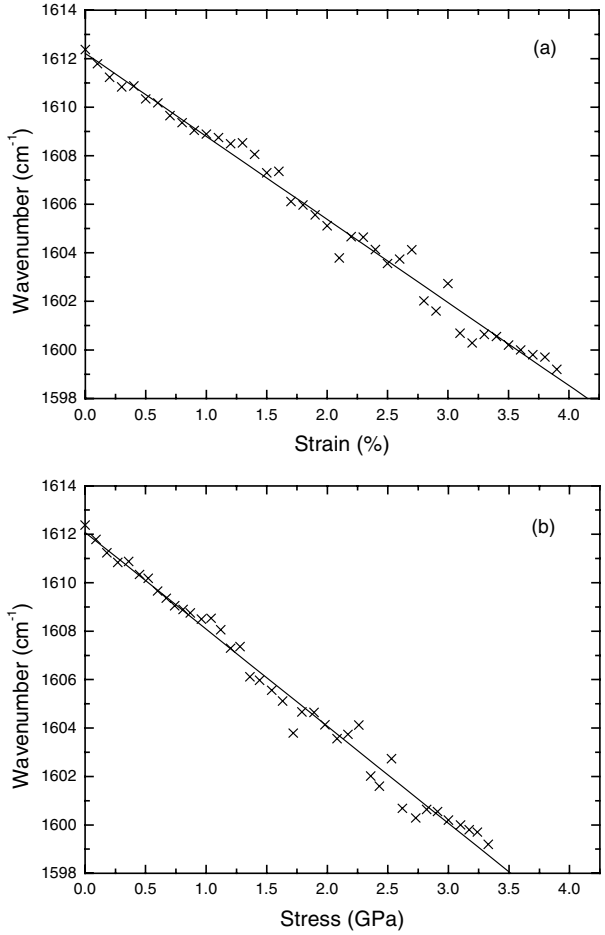

Figure 5 Relationships between Raman wavenumber and (a) tensile strain, (b) tensile stress for the Technora fibre.

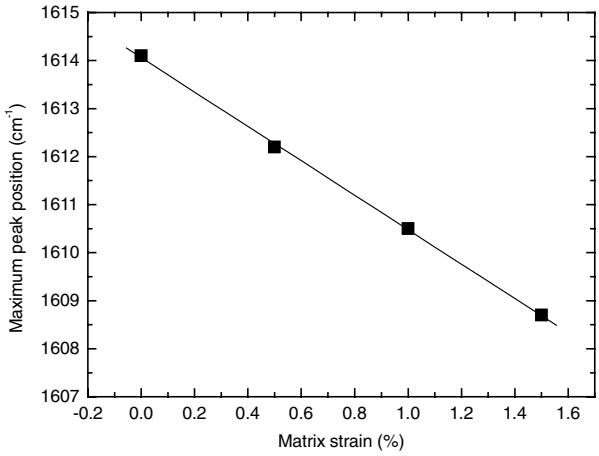

Figure 6 The shift of the 1613 cm^{-1} Raman band along the middle of Technora fibre embedded in the single fibre model composite.

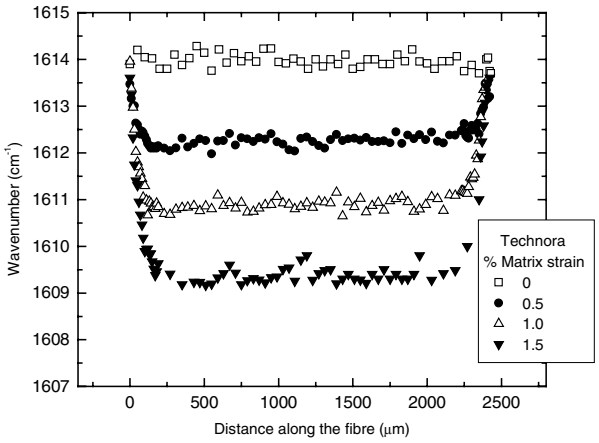

Figure 7 Variation of peak position of the 1613 cm^{-1} Raman band with the distance along the length of Technora fibre embedded in a single fibre model composite.

3.5. Interfacial characterisation

3.5.1. Dependence of Raman wavenumber upon matrix strain

From Fig. 6, it can be seen that the shift of the Raman band in the middle of the single fibre embedded in the composite (-3.6 ± 0.1 cm^{-1}/%) is similar to the shift of the free standing single fibre deformed in air (-3.6 cm^{-1}/%). This finding demonstrates clearly that Raman spectroscopy can be used as a tool to estimate the strain of the fibre in a single fibre embedded composite.

3.5.2. Variation of fibre strain along the length of the fibre embedded composite

The variation of Raman band position along the length of the fibre in the composite understress is shown in Fig. 7. The band positions were converted to fibre strain in the composite specimens by using the measured rate of shift of the Raman band with strain of the fibre in air (-3.6 cm^{-1}/%).

TABLE III XPS results of the Technora fibres showing atomic percentages of different elements in the fibre surfaces

Sample	%C	%O	%N	%Si	%Na	%P
Technora	81.3	13.1	1.5	3.4	0.6	0.2
Technora theoretical	78.8	9.1	12.1			

The stress transfer length (l_t) is defined as the length over which the strain in the fibre builds up to the plateau value [14] and the variations of stress transfer length obtained from averaging the values at both ends of the fibres are shown in Table IV. The stress transfer length was found to increase with increasing matrix strain. This is due to phenomena such as non-linear matrix deformation, yielding of the matrix or debonding that might occur locally at the interface around the fibre end leading to the increase of l_t especially at high strain levels. The large standard deviations show that there are some variations of the stress transfer length at each end of the fibres. This shows that care must be taken in the analysis of the behaviour of individual fibre ends. The scatter may be caused by damage at the cut fibre ends (causing the debonding to propagate along the end of the fibre) and the local variation of surface coating together with the wetting ability of the resin to the fibre ends. It may also be due to local variations in fibre structure affecting the elastic constant of the fibre, and imperfections at the interface induced when the composites were prepared.

3.5.3. Strength of the fibre-matrix interface

The strain distribution profiles of Technora fibres embedded composites were fitted using a logistic sigmoid

TABLE IV The average stress transfer length obtained from of both ends of 3 different specimens at various levels of matrix strain

Fibre	Average stress transfer length (μm) Matrix strain (%)		
	0.5	1.0	1.5
Technora	187 ± 60	245 ± 21	324 ± 46

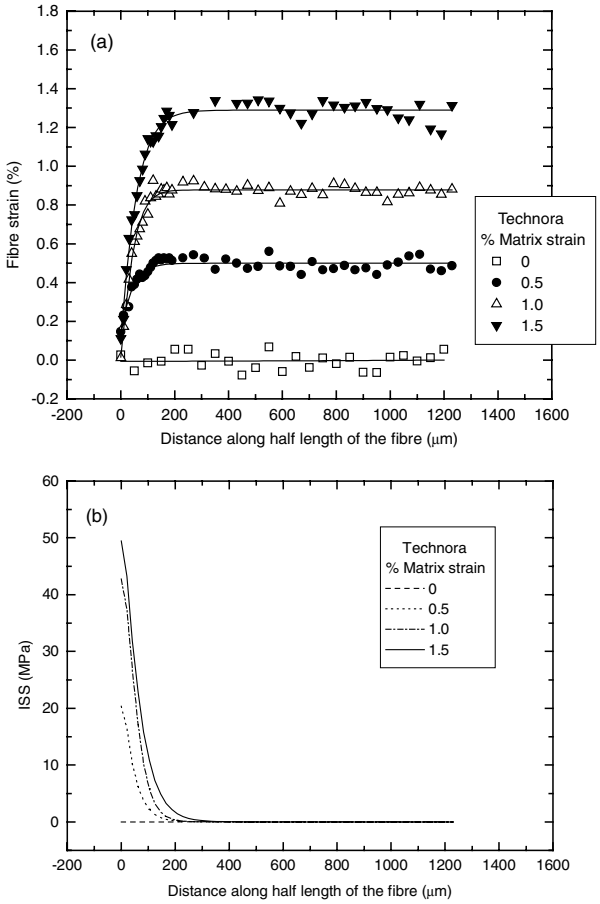

Figure 8 (a) Variation of fibre strain at the left-hand end of a Technora fibre embedded in a single fibre model composites fitted using the logisticsigmoid function. (b) Derived variation of ISS along the fibre-matrix interface.

function. Figs 8a and 9a show variations of fibre strain at the left and right hand ends of the Technora fibre, respectively. The experimental data fit well with a logistic sigmoid function (solid line) along the half length of the fibres. The fitted curves show a chi-squared value of about 0.001 at each strain level impling good fitting.

The interfacial shear stress (ISS) of the composites studied was calculated from

$$\tau = \frac{r_0}{2} E_f \left[\frac{\mathrm{d}e_f}{\mathrm{d}x} \right]$$

where τ is the interfacial shear stress, r_0 is the radius of the fibre, E_f is the fibre modulus and $\mathrm{d}e_f/\mathrm{d}x$ is the slope of the strain distribution curve along the length of the fibre. The value of $\mathrm{d}e_f/\mathrm{d}x$ was obtained from the derivative of the logistic sigmoidal fitted curves for all specimens. The variation of interfacial shear stress along the fibre-matrix interface at different level of matrix strain is shown in Figs 8b and 9b. It can be

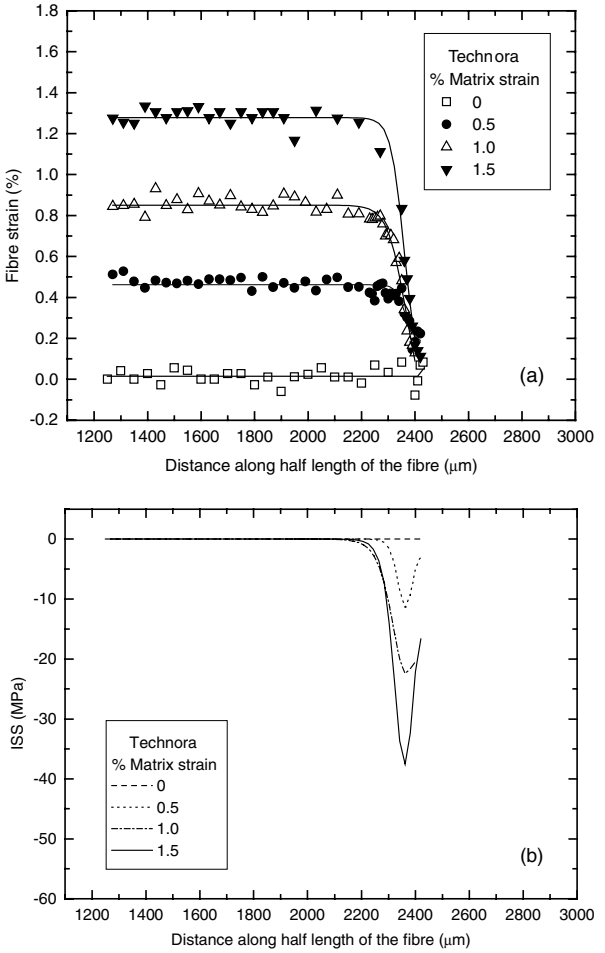

Figure 9 (a) Variation of fibre strain at the right-hand end of a Technora fibre embedded in a single fibre model composites fitted using the logisticsigmoid function. (b) Derived variation of ISS along the fibre-matrix interface.

seen generally that the value of ISS is highest at the fibre end and decreases to about zero at a certain length away from the end of the fibre. It also varies with matrix strain.

The maximum ISS or $\tau_{\max}$ is defined as the highest ISS measured at each strain level. It is generally found to occur near the fibre ends. The high value of $\tau_{\max}$ at the end of the fibre indicates that the high shear stress or stress concentration at the end of the fibre occurs before the failure of the interface takes place by further loading. It also implies a good bonding condition between the fibre and matrix interface. For some fibres, the $\tau_{\max}$ value appears at a distance x away from the end of the fibre. This indicates that debonding or yielding occured near the fibre end.

The different values of ISS obtained from the left and right hand ends (Figs 8b and 9b) are possibly due to the cut end damage and differences in cut end geometry. It would also be due to the variable wetting capability of the resin to the ends of the fibres and the variations of the diameter of the fibre. Summaries of $\tau_{\max}$ of the Technora fibre embedded composites are shown in Table V. It can be seen that the $\tau_{\max}$ values at the left hand ends are higher than those at the right hand ends for every matrix strain levels. This is probably due to stress relaxation during the experiments where measurements were taken starting at the left-hand end of

TABLE V Summaries of average maximum interfacial shear stresses of the Technora fibres

	% Matrix strain	Average max. ISS left end (MPa)	Average max. ISS right end (MPa)
Technora	0.5	18 ± 5	15 ± 4
	1.0	31 ± 4	23 ± 5
	1.5	46 ± 5	38 ± 3

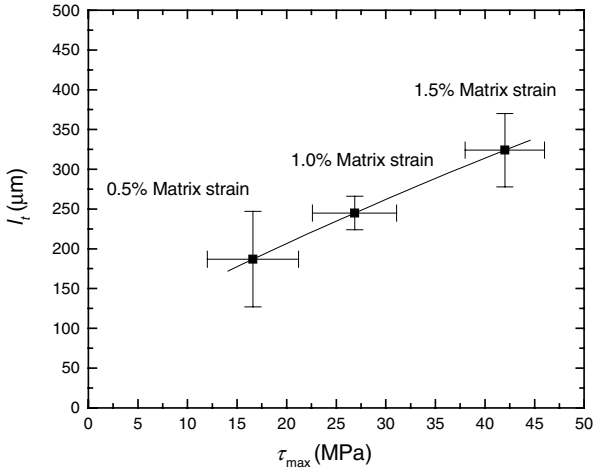

Figure 10 Relationships between l_t and τ_{max} for the Technora fibre composites.

the fibres. The range of values of τ_{max} (38–46 MPa) at high strain encompasses the matrix yield stress, which is about 43 MPa [5]. Previous work has shown that when adhesion at the interface is strong, the τ_{max} value is controlled by the shear yield stress of the matrix [5].

From Figs 8 and 9, it can be seen that the Technora fibre has good bonding with the resin matrix. It can be seen from Fig. 10 that the shorter the l_t value, the lower the averageτ_{max} value obtained from both fibre ends of the fibres studied. This indicates a good correlation between the value of l_t and τ_{max}.

4. Conclusions

Near-IR Raman spectroscopy can be successfully used to investigate variation of fibre strain and the interfacial adhesion along the length of the single fibre embedded composites for Techora fibres on an epoxy resin matrix. A sigmoid function can be used to fit to strain distribution profiles well at both ends of the fibres embedded in the fibre composites. The maximum ISS was found to be in the range 38–46 MPa, similar to the shear yield stress of the matrix demonstrating that the standard Technora fibre finish may provide adequate bonding between the fibres and an epoxy resin matrix.

Acknowledgements

The authors are grateful to Teijin-Twaron Ltd. for the supply of the Technora fibres and to Corrosion and Protection Centre of the School of Materials for help with the XPS measurements. One of the authors (W.P.) is also grateful to the Government of Thailand for supporting the form of a Scholarship.

References

1. H. H. YANG, "Aromatic High Strength Fibers" (John Wiley & Sons, New York, 1989).
2. H. JAHANKHANI and C. GALIOTIS, *J. Comp. Mater.* **25** (1991) 609.
3. C. GALIOTIS, *Comp. Sci. Technol.* **42** (1991) 125.
4. M. C. ANDREWS, R. J. DAY, X. HU and R. J. YOUNG, *ibid.* **48** (1993) 255.
5. M. C. ANDREWS, Stress transfer in aramid/epoxy model composites. PhD Thesis, UMIST, 1994.
6. J. A. BENNETT and R. J. YOUNG, *Comp. Sci. Technol.* **57** (1997) 945.
7. A. J. CERVENKA, D. J. BANNISTER and R. J. YOUNG, *Composites: Part A* **29A** (1998) 1137.
8. D. N. BATCHELDER and D. BLOOR, *J. Polymer Sci.: Polymer Phys.* **17** (1979) 569.
9. M. G. NORTHOLT and J. J. V. AARTSEN, *J. Polymer Sci.: Polymer Symposia* **58** (1977) 283.
10. W. Y YEH, Structure-property relationships in engineering polymer fibres. PhD Thesis, UMIST, 1995.
11. N. B. COLTHUP, L. H. DALY and S. E. WIBERLEY, "Introduction to Infrared and Raman Spectroscopy" 3rd Ed. (Academic Press Inc, London, 1990).
12. W. Y. YEH and R. J. YOUNG, *Polymer* **40** (1999) 857.
13. J. CHASTAIN and R. C. KING, "Handbook of X-ray Photoelectron Spectroscopy" (Physical Electronics, Inc., USA, 1995).
14. D. HULL and T. W. CLYNE, "An Introduction to Composite Materials" (Cambridge University Press, Cambridge, 1996).

Received 10 June 2004
and accepted 14 February 2005